An Unlikely Sugar Substrate Site in the 1.65 Å Structure of the Human Aldose Reductase Holoenzyme Implicated in Diabetic Complications

David K. Wilson, Kurt M. Bohren, Kenneth H. Gabbay, Florante A. Quiocho*

Aldose reductase, which catalyzes the reduced form of nicotinamide adenine dinucleotide phosphate (NADPH)–dependent reduction of a wide variety of aromatic and aliphatic carbonyl compounds, is implicated in the development of diabetic and galactosemic complications involving the lens, retina, nerves, and kidney. A 1.65 angstrom refined structure of a recombinant human placenta aldose reductase reveals that the enzyme contains a parallel β8/α8-barrel motif and establishes a new motif for NADP-binding oxidoreductases. The substrate-binding site is located in a large, deep elliptical pocket at the COOH-terminal end of the β barrel with a bound NADPH in an extended conformation. The highly hydrophobic nature of the active site pocket greatly favors aromatic and apolar substrates over highly polar monosaccharides. The structure should allow for the rational design of specific inhibitors that might provide molecular understanding of the catalytic mechanism, as well as possible therapeutic agents.

Aldose reductase (E.C. 1.1.1.21) catalyzes the NADPH-dependent reduction of a wide variety of carbonyl-containing compounds to their corresponding alcohols with a broad range of catalytic efficiencies. The k_{cat}/K_m values (k_{cat}, catalytic constant; K_m, Michaelis constant) of aldose reductase are in the range of 10^4 to 10^5 s^{-1} M^{-1} for a number of aromatic and hydrophobic compounds (*1*). Several polar hexose sugars are the least favored and nonspecific substrates, exhibiting k_{cat}/K_m values of ~1 s^{-1} M^{-1} (*1*). The enormous differences in catalytic efficiency between hydrophobic and polar substrates are highly correlated to differences in K_m values ($<10^{-6}$ M for steroids to 10^{-1} M for glucose).

A normal physiological role for the enzyme has not been established, but its ability to reduce the excess glucose resultant from the hyperglycemia of diabetes mellitus is believed to be linked to diabetic complications affecting the lens, retina, peripheral nerves, and kidney (*2*). A variety of nonspecific planar aromatic inhibitors of the enzyme have been shown to be effective in preventing some of the complications in animal models but were found to be either ineffective or toxic in clinical studies (*3*).

The recombinant human aldose reductase consists of a single polypeptide chain of 315 residues with a molecular mass of 35.8 kD (*4*). We have obtained crystals of the purified holoenzyme that diffract to 1.5 Å (*5*). The phases, solved by combined single isomorphous replacement and anomalous scattering from a three-site uranyl derivative, yielded a high-quality electron density map with a resolution of 2.5 Å to which all but the last 30 residues of the amino acid sequence were fitted readily. A complete atomic model of the enzyme and a bound NADPH were obtained in the course of several cycles of model building with the CHAIN program (*6*) and with refining the atomic coordinates with the XPLOR package (*7*). Ultimately, the structure refinement of the entire coordinates, which consisted of 2517 nonhydrogen protein atoms, 48 NADPH atoms, and 95 solvent atoms, was carried out against the 1.65 Å resolution x-ray data to an *R* factor of 0.20. A complete description of the structure determination and the model will appear elsewhere.

Aldose reductase folds into a β/α or triosephosphate isomerase barrel with a core of eight parallel β strands (Fig. 1). Adjacent strands are connected by eight peripheral α-helical segments running antiparallel to the β sheet. This general motif is similar to those found in approximately two dozen enzymes (*8*) that are unrelated in primary sequences and functions, several requiring cofactors including the Fe-S cluster, metal, flavin, and heme, and now NADPH for aldose reductase. The aldose reductase structure is completely different from other reductases such as the dihydrofolate reductase and the superfamily typically represented by glutathione reductase (*9*) as it is, to our knowledge, the first NADPH/NADH–dependent oxidoreductase with solely a β/α-barrel motif.

Several secondary structure elements break up the regularity of the $(\beta/\alpha)_8$ barrel of aldose reductase (Fig. 1). The first strand (β1) of the barrel is preceded by a β-hairpin turn that lies across the NH_2-terminal end of the β barrel. There are also two auxiliary helices (H1 and H2), one preceding α7 and the other following α8, that are packed parallel to each other. The 24-residue, COOH-terminal peptide meanders from the end of H2 on the NH_2-terminal side of

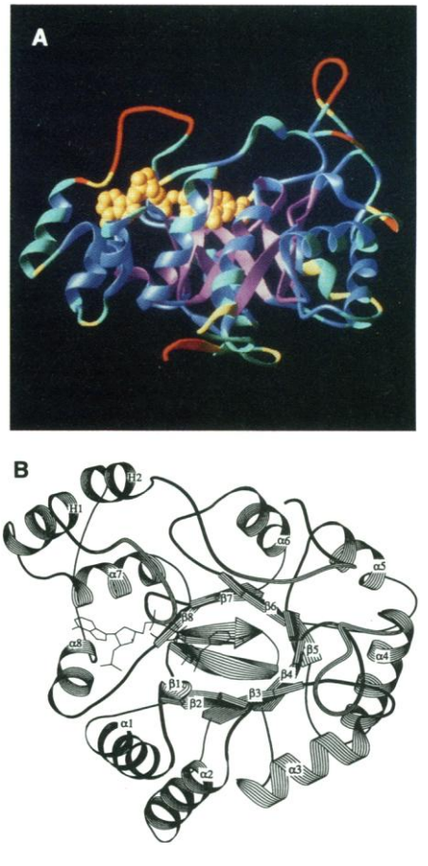

Fig. 1. Perspective view of the α-carbon backbone trace (schematic diagram) of the aldose reductase structure with bound NADPH. (**A**) The enzyme viewed perpendicular to the β/α barrel with the NADPH shown in yellow space-filling model. The colors of the backbone trace only represent the temperature factor of the α carbons: purple, isotropic *B* values below 5 Å^2; blue, between 5 and 10 Å^2; green, between 10 and 15 Å^2; yellow, between 15 and 20 Å^2; and red, greater than 20 Å^2. As a whole the β-strand core of the barrel has the lowest average *B* factor that then increases radially. Two loops with red color (residues 122 to 132, top right, and residues 214 to 228, top left) protruding above the active site have the highest average *B* factors. The loop of residues 214 to 228 folds over the pyrophosphate bridge of NADPH (see text and also Fig. 2C). Figure drawn with the program RIBBONS (*22*). (**B**) The structure viewed down the COOH-terminal end of the β barrel with the NADPH molecule drawn in stick model. The eight α helices and eight β strands associated with the barrel are identified. The two extra helices are labeled H1 and H2. Figure drawn with the program RIBBON (*23*).

D. K. Wilson and F. A. Quiocho, Howard Hughes Medical Institute and Department of Biochemistry, Baylor College of Medicine, Houston, TX 77030.
K. M. Bohren and K. H. Gabbay, Departments of Pediatrics and Cell Biology, Baylor College of Medicine, Houston, TX 77030.
*To whom correspondence should be addressed.

the molecule to the top of the COOH-terminal end of the β barrel.

As observed in all other β/α-barrel enzymes (8), the active site of aldose reductase is located at the COOH-terminal end of the β barrel (Fig. 1). In this site is a large, deep, elliptical cavity, bounded mainly by the termini of the β strands and loops, wherein the nicotinamide ring of the NADPH cofactor and the substrate binding site are found. As might be expected of a structure refined at 1.65 Å, the electron density of the NADPH (Fig. 2A) and the residues in the cavity, and indeed of the entire protein molecule, are well resolved.

The NADPH is bound in an unusual extended conformation across the barrel with the nicotinamide ring centered in the deep part of the active site cavity and the adenosine-2′-monophosphate wedged in a shallow depression outside the β barrel, between a couple of β strands and α helices (Fig. 1). The pyrophosphate bridge of NADPH straddles the lip of the barrel. Relative to the ribose moiety, both the nicotinamide and the adenine adopt the anti conformation. The NADPH is held in place by a total of 19 hydrogen bonds and three salt links (Fig. 2B).

The bound NADPH is barely accessible to solvent (Fig. 2C); the accessible surface areas, as defined by Lee and Richards (*10*), of 20.0 $Å^2$ of the bound NADPH represent only about 7.5% of the accessible area of the corresponding free coenzyme. The C-4 carbon of the bound nicotinamide is the only atom of that ring that retains any solvent accessibility. The remaining solvent-accessible atoms are contained in the adenosine monophosphate (AMP) moiety.

The partial stacking of the A face (*11*) of the nicotinamide ring against Tyr^{209} (Figs. 2A and 3) located in the bottom of the active site pocket is largely responsible for orienting the ring and in making that face completely inaccessible. Similar stacking interactions have also been observed in a number of dehydrogenases and reductases. The orientation of the B face of the nicotinamide group toward the opening of the cavity (Fig. 3) is consistent with the finding that the axial 4-*pro*-*R* hydrogen of the nicotinamide is transferred to substrates (*12*). The nicotinamide is further held in place by hydrogen bonding of the amide group with Gln^{183}, Asn^{160}, and Ser^{159} residues. These interactions orient the nicotinamide ring so that the 4-*pro*-*R* hydrogen is always directed toward the opening of the pocket.

All of the residues making hydrogen-bonding and charge-coupling interactions with the polar groups of the adenosine-2′-monophosphate come from an 11-residue loop (residues 262 to 272) (Fig. 2B). The faces of the adenine ring are exposed to two different environments; the A face is close to Arg^{268}, whereas the B face abuts Leu^{212} and Leu^{228}. The adenosine mononucleotide is firmly secured by the interactions with its 2′-phosphate group (Fig. 2B). The phosphate forms four hydrogen bonds with three residues (two hydroxyl side chains and one main chain NH) and one water. It is also involved in salt-linking and hydrogen-bonding interactions with the side chains of Lys and Arg residues. These interactions account for the observed preference of NADPH over NADH (*1*).

The placement and interaction of the pyrophosphate bridge of NADPH are intriguing. The pyrophosphate, along with parts of the flanking ribose units, is threaded through a short tunnel (Fig. 2C) with one side occupied by residues 213 to 217 that initiate a loop of residues from 213 to 227. The other side is lined with residues Trp^{20}, Lys^{21}, Pro^{261}, and Lys^{262}. These residues and the loop fold over the pyrophosphate and are mainly held together in a fashion akin to a safety belt or drawbridge by the salt links between Asp^{216} on one side and Lys^{21} and Lys^{262} on the opposite side.

With the pyrophosphate tied down by

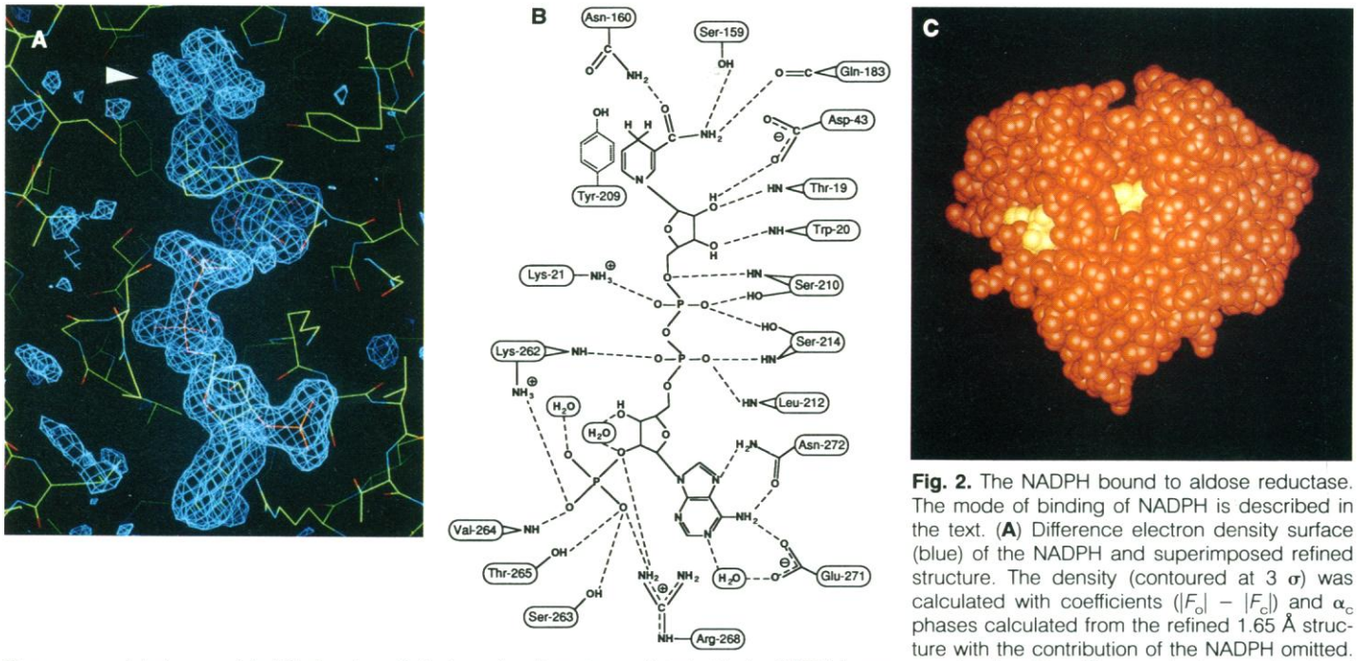

Fig. 2. The NADPH bound to aldose reductase. The mode of binding of NADPH is described in the text. (**A**) Difference electron density surface (blue) of the NADPH and superimposed refined structure. The density (contoured at 3 σ) was calculated with coefficients ($|F_o| - |F_c|$) and α_c phases calculated from the refined 1.65 Å structure with the contribution of the NADPH omitted. The arrow points to an unidentified region of electron density not associated with the NADPH or water molecules. The difference in electron density of this region on average is only about 50% of the NADPH density. Immediately to the left of the nicotinamide ring is Tyr^{209} that partially stacks against the A face of the ring. To the right and above the ring are Tyr^{48} and His^{110}, respectively, that are potential hydrogen donors in the mechanism. (**B**) Schematic diagram of the hydrogen-bonding and salt-linking interactions between aldose reductase and NADPH. Also depicted is the partial stacking of the nicotinamide ring against Tyr^{209}. (**C**) Space-filling model of the nonhydrogen atoms of the aldose reductase structure (red) and the NADPH (yellow) with an orientation similar to Fig. 1B. A portion of the nicotinamide (center) is seen in the substrate-binding pocket. To the left of that is the 5′-phosphate and a part of a ribose of the adenosine. The pyrophosphate bridge of the NADPH is hidden or made inaccessible by a "drawbridge" or "safety belt" with one section consisting of residues 21, 22, 262, and 263 and the other section made up of the loop of residues 214 to 228 (Fig. 1). A conformational change, possibly a drawing up and down of the loop section, is necessary for the association and dissociation of the NADPH.

the safety belt, dissociation of the NADPH would require a conformational change. This change can be accomplished by a hinged flap or lid motion of the loop of residues Gly^{213} to Leu^{227}, which is akin to those suggested for other barrel enzymes (8, 13). This loop (excluding the residues involved in salt links) has an average thermal motion that is one of the highest of the entire backbone (Fig. 1). The finding that the NADPH is tightly held in place by the belt and by the large number of hydrogen bonds, salt linkages, and van der Waals contacts provides a structural basis for the slow release of the coenzyme in the catalytic reaction sequence (14).

In addition to one salt link to Lys^{262}, the pyrophosphate makes five hydrogen bonds (Fig. 2B). The two oxygens of one of the phosphoryl units are involved solely in charge-dipole interactions with three-peptide-unit NH groups. Similar charge stabilization by local dipoles (including those of hydroxyl groups) of otherwise uncompensated ionic groups have been observed in a number of proteins (15).

The presence of the nicotinamide ring, with its exposed B face, at the bottom of the elliptical pocket dictates the location of the active site of aldose reductase (Fig. 3). An as-yet-unidentified region of weak electron density sits on top of the B face or accessible side of the nicotinamide ring where the substrate or product would presumably be found. As can be seen in Fig. 2A, the density in the ($|F_o| - |F_c|$, α_c) map is not as well defined as that of the NADPH difference density, indicating that it is either disordered or a composite of unknown ligands. Attempts made at modeling and refining carbon atoms in the density were unsuccessful.

The pocket (Fig. 3), with a depth of about 12 Å and a base of about 7 by 13 Å, is very hydrophobic, being lined by seven aromatic residues (Trp^{20}, Tyr^{48}, Trp^{79}, Trp^{111}, Phe^{121}, Phe^{122}, and Trp^{219}) and four apolar

Table 1. Crystallographic and refinement data. The resolution for the native crystals is 1.65 Å, and for the $K_2UO_2F_5$-soaked crystals was 2.5 Å. Definitions: R merge is the R factor on intensities for merging symmetry-related reflections; R Cullis = $\Sigma \| F_{PH} \pm F_P | - F_H | \Sigma | F_{PH} - F_P |$, where the structure factors are for the protein (F_P), the heavy atom (F_H), or their complex (F_{PH}); R anom (rms) = $[\Sigma(\Delta F_O^{\pm} - \Delta F_C^{\pm})^2 / \Sigma(\Delta F_O^{\pm})^2]^{1/2}$, where F_O is the observed and F_C is the calculated structure factor; and R factor = $\Sigma | F_O - F_C | / \Sigma | F_O |$; I is the intensity, where σ_I is the standard deviation of the intensity.

Parameter	Crystal	
	Native	$K_2UO_2F_5$
Diffraction data		
Observations (no.)	128,951	76,568
Reflections (no.)	35,859	20,201
Completeness of data (%)	92.7	98.4
$<I>/\sigma_I$	22.6	25.1
R merge (%)	4.5	5.6
Phasing and structure refinement statistics		
Isomorphous differences (no.)		10,363
Anomalous differences (no.)		8,406
F_H/residual (rms)		3.49
R Cullis		0.43
R anom		0.40
Figure of merit		0.74
R factor	0.20	
Bond deviation from ideality (Å) (rms)	0.014	
Angle deviation from ideality (°) (rms)	3.13	

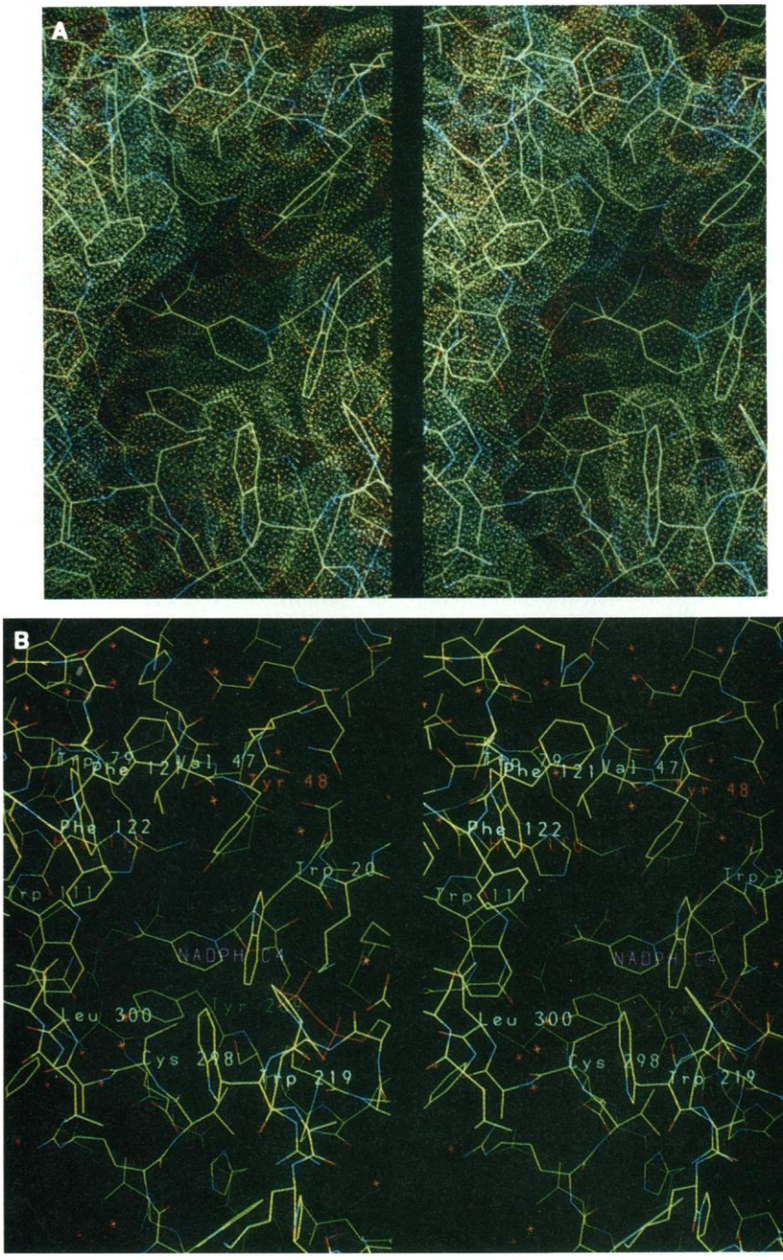

Fig. 3. A stereo view of the large, deep, elliptical active site pocket with the nicotinamide ring lying at the bottom of the pocket. Clearly shown are many of the aromatic and aliphatic side chains that line the pocket. (**A**) The individual van der Waals radii used for the atomic surfaces were C = 1.7 Å (green), N = 1.6 Å (blue), and O = 1.5 Å (red). The pocket has a depth of about 10 Å and a base of about 7 Å by 13 Å. (**B**) Similar to (A) but without the dot atomic surfaces. Many of the aromatic and aliphatic residues that line the pocket are identified in light green and with residue numbers. The C-4 carbon of the nicotinamide is labeled in purple. The two possible hydrogen donors, Tyr^{48} and His^{110}, in the catalytic mechanism are shown in red.

residues (Val^{47}, Pro^{218}, Leu^{300}, and Leu^{301}). Many of the aromatic residues are depicted in Fig. 3. Gln^{49}, Cys^{298}, and His^{110} are the only polar side chains lining the pocket; the Gln residue is located on the rim of the pocket, whereas the Cys and His residues are within 4 Å of the nicotinamide ring.

The large size and extremely hydrophobic nature of the active site pocket are consistent with the observations that aromatic compounds (such as isocorticosteroids) are the best substrates of aldose reductase (*1*). The active site pocket is not designed for binding sugars with high specificity and affinity, as seen in all other known structures of proteins (including enzymes) that bind carbohydrates (*16*). This is fully consistent with the observations that a variety of hexoses are extremely poor substrates of the aldose reductase. With the exception of one histidine, the active site of the reductase is devoid of polar residues that confer, through hydrogen bonds, the high specificity and affinity of all the other carbohydrate-binding proteins (*16*).

The catalytic mechanism of aldose reductase appears to be relatively simple, consisting of a stereospecific transfer of the 4-*pro-R* hydrogen from the exposed C-4 of the nicotinamide to the carbon of the carbonyl group of the substrate and abstraction of a hydrogen from a donor group by the incipient negatively charged carbonyl oxygen. Assuming that the location of the substrate's reactive carbonyl group is close to the C-4 of the nicotinamide, we see only three residues that are potential sources of the requisite hydrogen—Tyr^{48}, His^{110}, or Cys^{298} (Figs. 2A and 3). The hydroxyl of Tyr^{48}, the nitrogen Nε of His^{110}, and the SH of Cys^{298} are at a distance of 4.52, 5.12, and 4.13 Å, respectively, of the C-4. Either Tyr^{48} or His^{110} could be the hydrogen donor (Fig. 3B) because both residues are conserved in the enzyme superfamily, whereas Cys^{298} is not conserved. From a structural point of view, Tyr^{48} is favored because the hydrogen-bonding interaction of its hydroxyl group with the ammonium side chain of Lys^{77} (Fig. 3B), which is in turn salt-linked with Asp^{43}, would help facilitate hydrogen transfer. His^{110} is less favored because it is close to three hydrophobic residues (Trp^{79}, Val^{47}, and Trp^{111}) and, hence, is likely to have an abnormally low pK_a, the negative logarithm of the acid constant. It would then be predominantly unprotonated at about pH 6.5 where aldose reductase exhibits maximum activity (*1*).

A variety of inhibitors of aldose reductase, most consisting of a planar aromatic ring system with an electrophilic group, are not specific for the enzyme (*17*). Nevertheless, some inhibitors have been shown to be effective in preventing some of the complications due to diabetes in animal models but were either ineffective or toxic in clinical studies (*3*). To date, there are no known competitive inhibitors, and kinetic studies of a variety of compounds show uncompetitive inhibitions indicating that the inhibitors bind at a site independent of that of the substrate or the cofactor (*18*). As the inhibitors rely chiefly on hydrophobic interactions, these endow them with the ability to bind nonspecifically in the hydrophobic pockets equally well in other proteins or enzymes.

A 2.2 Å electron density map generated from data collected from a crystal of aldose reductase soaked in 1.3 mM tolrestat, an uncompetitive inhibitor (inhibition constant in the nanomolar range) that is being clinically tested and even marketed (*19*), did not clearly reveal an inhibitor-binding site. A well-designed specific inhibitor of aldose reductase should make use of the shape and hydrophobic nature of the pocket as well as the few polar groups in it. The aldose reductase structure establishes the general motif for a number of other enzymes with which it shares significant sequence similarities, namely aldehyde reductase, prostaglandin F synthase, frog ρ crystallin, 2,5 diketogluconic acid reductase, and chlordecone reductase (*4*, *20*, *21*). Our sequence comparison of these proteins shows that most of the critical NADPH binding residues are conserved across all or most of these enzymes. The residues in the substrate-binding pocket in the aldose reductase, however, are less conserved across the rest of the proteins. Although the enzyme has been implicated with diabetic complications, it has an unlikely binding site for hexoses—the very substrates that are believed to be responsible in the pathogenesis of these complications.

REFERENCES AND NOTES

1. B. Wermuth, H. B. Bürgisser, K. M. Bohren, J-P. von Wartburg, *Eur. J. Biochem.* **127**, 279 (1982); B. Wermuth, in *Enzymology of Carbonyl Metabolism: Aldehyde Dehydrogenase, Aldo/Keto Reductase and Alcohol Dehydrogenase*, H. Weiner and B. Wermuth, Eds. (Liss, New York, 1992), pp. 261–274.
2. K. Gabbay, *N. Engl. J. Med.* **288**, 831 (1973); P. F. Kador, *Med. Res. Rev.* **8**, 325 (1988).
3. D. M. Dvornik *et al.*, *Science* **182**, 1146 (1973); C. N. Martyn, W. Reid, R. J. Young, D. J. Ewing, G. F. Clark, *Diabetes* **36**, 987 (1987); S. P. Spielberg, N. H. Shear, M. Cannon, N. J. Hutson, K. Gunderson, *Ann. Intern. Med.* **114**, 720 (1991).
4. K. M. Bohren, B. Bullock, B. Wermuth, K. H. Gabbay, *J. Biol. Chem.* **264**, 9547 (1989); K. M. Bohren, J. L. Page, R. Shankar, S. P. Henry, K. H. Gabbay, *ibid.* **266**, 24031 (1991).
5. We obtained crystals by suspending a droplet containing protein (14 mg/ml), 50 mM citrate, and 7 mM β-mercaptoethanol in various concentrations of polyethylene glycol (PEG) 6000 over 20% PEG in the same buffer at a pH of 5.0. Seeding was used to improve the size of the crystals. The crystals belong to the space group $P2_12_12_1$ with unit cell dimensions of a = 50.00 Å, b = 67.12 Å, and c = 92.02 Å and one molecule per asymmetric unit. They diffract x-rays to at least 1.5 Å on a rotating anode (CuK_α source operated at 40 kV and 110 mA) equipped with an ADSC multiwire two-area detector system.
6. J. S. Sack, *J. Mol. Graphics* **6**, 224 (1988).
7. A. T. Brünger, *XPLOR, A System for Crystallography and NMR, 2.1 Manual* (Yale University, New Haven, CT, 1990).
8. C.-I. Branden, *Curr. Opin. Struct. Biol.* 1, 978 (1991); G. K. Farber and G. A. Petsko, *Trends Biochem. Sci.* **15**, 228 (1990).
9. J. T. Bolin, D. J. Filman, D. A. Matthews, R. C. Hamlin, J. Kraut, *J. Biol. Chem.* **257**, 13650 (1982); J. Kuriyan *et al.*, *Nature* **352**, 172 (1991); E. F. Pai, *Curr. Opin. Struct. Biol.* 1, 796 (1991).
10. B. Lee and F. M. Richards, *J. Mol. Biol.* **55**, 379 (1971). The program ACCESS used to calculate solvent accessibility was provided by F. M. Richards.
11. We have adopted the proposal by Rose *et al.* [I. A. Rose, K. R. Hanson, K. D. Wilkinson, M. J. Wimmer, *Proc. Natl. Acad. Sci. U.S.A.* **77**, 2439 (1980)] for distinguishing between the two faces of an asymmetric aromatic ring (for example, adenine and nicotinamide) as A face and B face, in which the numbering of the atoms increases in a clockwise and counterclockwise direction, respectively.
12. H. B. Feldman *et al.*, *Biochim. Biophys. Acta* **480**, 18 (1977).
13. D. Joseph, G. A. Petsko, M. Karplus, *Science* **249**, 1425 (1990); D. K. Wilson, F. B. Rudolph, F. A. Quiocho, *ibid.* **252**, 1278 (1991).
14. C. E. Grimshaw, M. Shahbaz, C. G. Putney, *Biochemistry* **29**, 9947 (1990).
15. H. Luecke and F. A. Quiocho, *Nature* **347**, 402 (1990); F. A. Quiocho, J. S. Sack, N. K. Vyas, *ibid.* **329**, 561 (1987).
16. F. A. Quiocho, *Annu. Rev. Biochem.* **55**, 287 (1986); *Pure Appl. Chem.* **61**, 1293 (1989); H. M. Einspahr, Ed., Proceedings of the Symposium on Protein-Carbohydrate Interactions, *Transaction of the American Crystallographic Association*, (1989), vol. 25; N. K. Vyas, *Curr. Opin. Struct. Biol.* 1, 732 (1991).
17. M. M. O'Brien, P. J. Schofield, M. R. Edwards, *J. Neurochem.* **39**, 810 (1982); P. F. Kador, W. G. Robison, J. H. Kinoshita, *Annu. Rev. Pharmacol. Toxicol.* **25**, 691 (1985); R. Poulsom, *Biochem. Pharmacol.* **35**, 2955 (1986).
18. C. E. Grimshaw *et al.*, *Biochemistry* **28**, 5343 (1989).
19. A. Bhatnagar, S. Q. Liu, B. Das, N. H. Ansari, S. K. Srivastava, *Biochem. Pharmacol.* **39**, 1115 (1990); A. J. Boulton, S. Levin, J. Comstock, *Diabetologia* **33**, 431 (1990).
20. S. Anderson *et al.*, *Science* **230**, 144 (1985); S. I. Tomarev *et al.*, *FEBS Lett.* **171**, 297 (1984); K. Watanabe *et al.*, *Proc. Natl. Acad. Sci. U.S.A.* **85**, 11 (1988); C. J. Winters, D. T. Molowa, P. S. Guzelian, *Biochemistry* **29**, 1080 (1990).
21. After submission of this paper, a paper describing the 2.5 Å structure of pig lens aldose reductase appeared [J.-M. Rondeau *et al.*, *Nature* **355**, 469 (1992)]. Although the structures of the human and pig enzymes are similar, the following are described herein for the first time: the precise mode of binding and sequestering of NADPH, the stereochemistry of hydrogen transfer from the coenzyme, the location and extremely hydrophobic nature of the active site, and the two possible residues important for the catalytic mechanism.
22. M. Carson, *J. Mol. Graphics* **5**, 103 (1987).
23. J. Priestle *ibid.* **21**, 572 (1988).

24. We thank T. Reynolds and C. Wallace for assistance in preparing the manuscript. Supported by the Howard Hughes Medical Institute and the W. M. Keck Foundation (F.A.Q.) and by grants from NIH (DK-39,044) (K.H.G.), the Juvenile Diabetes Foundation (1901111) (K.M.B.), (1891113) (K.H.G.), and the Harry B. and Aileen B. Gordon Foundation (K.H.G.). Coordinates will be deposited in the Brookhaven Protein Data Bank.

28 January 1992; accepted 5 May 1992